

Stable pinching by controlling finger relative orientation of robotic fingers with rolling soft tips

Efi Psomopoulou[†], Daiki Karashima[‡], Zoe Doulgeri^{†*} and Kenji Tahara[‡]

[†]*School of Electrical and Computer Engineering, Aristotle University of Thessaloniki, 54124 Thessaloniki, Greece. E-mail: efipsom@eng.auth.gr*

[‡]*Faculty of Engineering, Kyushu University, Fukuoka 819-0395, Japan. E-mails: karashima@hcr.mech.kyushu-u.ac.jp, tahara@mech.kyushu-u.ac.jp*

(Accepted June 27, 2017. First published online: August 14, 2017)

SUMMARY

There is a large gap between reality and grasp models that are currently available because of the static analysis that characterizes these approaches. This work attempts to fill this need by proposing a control law that, starting from an initial contact state which does not necessarily correspond to an equilibrium, achieves dynamically a stable grasp and a relative finger orientation in the case of pinching an object with arbitrary shape via rolling soft fingertips. Controlling relative finger orientation may improve grasping force manipulability and allow the appropriate shaping of the composite object consisted of the distal links and the object, for facilitating subsequent tasks. The proposed controller utilizes only finger proprioceptive measurements and is not based on the system model. Simulation and experimental results demonstrate the performance of the proposed controller with objects of different shapes.

KEYWORDS: Stable pinching; Relative finger orientation; Soft rolling contact; Feedback control.

1. Introduction

More than a few multi-fingered robot hands have been built since the early robotics research years in order to resemble the human hand^{1–5} and some are now commercially available for research purposes, but most of them sacrifice degrees of freedom (DOF) and thus dexterity for compactness and lightweight structure. However, grasp stability and manipulation dexterity is irrevocably connected with the rolling ability of human fingertips as it allows fine and accurate adjustment of contact positions.^{6,7} The progress accomplished in the last decades regarding grasp planning and control is shown in several review papers,^{8–10} but it is not adequate to resolve the grasping problem in uncertain and dynamic environments which is still considered as one of the main challenges that need to be solved for home robots.¹¹

The first approaches to grasp planning were analytical methods to synthesize force closure grasps and are based on accurate models of the hand kinematics, the object and their relative alignment.^{12–15} However, precise geometric and physical object model availability is not always the case in practice. Moreover, surface properties or friction coefficients, weight, center of mass, and weight distribution may not be usually known. Last, systematic and random errors occur in real robotic systems due to robot inaccurate models and noisy sensors. Consequently, real-world applications of grasps synthesized analytically may fail. Despite relaxing some of the assumptions,^{16,17} analytical methods are still mainly validated in simulations^{18,19} or consider 2D objects.^{19–21}

In the last decade, the availability of grasp planning simulators, like GraspIt!,²² made data-driven methods become popular. These approaches rely on sampling grasp candidates from some knowledge base and rank them according to a specific metric.^{23–27} Grasp parameterization is less

* Corresponding author. E-mail: doulgeri@eng.auth.gr

specific in these methods; in fact, they utilize an object grasping point with which the tool center point should be aligned, an approach vector instead of fingertip position, wrist orientation and initial finger configuration. Consequently, these approaches are robust to perception and execution uncertainties. However, as the simulated environment does not resemble the real world adequately, grasp success is not guaranteed during execution. In fact, studies have showed that grasps synthesized with data-driven methods under-performed significantly in practice, when compared with grasps kinesthetically taught by humans.^{28,29}

The large gap between reality and grasp models that are currently available is owed to the static analysis that characterizes all the above approaches. Although force closure implies the existence of an equilibrium, this is not sufficient for ensuring grasp stability,^{13,14} as it was shown in recent works, physics-based dynamical simulations are a more reliable way to rate a grasp success.^{30,31} The need for further studying grasp dynamics and developing analytical models that better resemble reality is identified in Bohg *et al.* [10]. An approach to bridging the gap between reality and models, is the design of model free grasp controllers that dynamically achieve a stable grasp equilibrium state. Previous research work in this direction includes feedback control laws of low complexity that consider rolling contacts.^{32–34} This class of controllers achieves stable grasping and fine manipulation without any force and contact sensing requirements for objects with flat surfaces and arbitrary shape for both the 2D and 3D cases.^{7,35–41} As the initial finger-object pose and contact positions must not necessarily correspond to an equilibrium state, perception and execution errors can be accommodated.

This work belongs to the previously mentioned class of controllers that achieve dynamically a stable grasp equilibrium state. It considers the 2D case of pinching of an object with two soft-tip robotic fingers while adjusting the relative finger orientation. The two objectives are considered in a single design producing one control signal in contrast with previous works where multiple control signals are superimposed to achieve each objective. The relative finger orientation feature is required when the volume of the finger-object composite needs to be adjusted for subsequent placement of the object in a constrained environment or for increasing the grasping force manipulability. The proposed control law allows pinching of an arbitrary-shaped object as it does not require any knowledge of the contact normals, uses only proprioceptive measurements, and is proved to attain a stable equilibrium state by fingertip rolling motions. A preset desired grasping force is further achieved and the relative finger orientation is adjusted with the use of a tunable control parameter. Preliminary results of this work are reported in Grammatikopoulou *et al.* [41] for fingers with rigid tips. In this work, the proposed controller and its stability are analyzed for the more realistic soft fingertip case and is extensively validated by both simulations and experiments conducted on a prototype robotic hand setup with various object shapes.

The rest of the paper is organized as follows. Section 2 states the basic assumptions considered as well as the kinematics and dynamics of the system. Section 3 presents the proposed grasping control law, while Sections 4 and 5 analyze the system equilibrium and its stability. Simulation studies are conducted in Section 6 and experimental results are presented in Section 7. Finally, conclusions are drawn in Section 8.

2. System Modeling

The system consists of two three-DOF robotic fingers with revolute joints and soft hemispherical tips of radius $r_1 = r_2 = r$ in the x - y plane. The following assumptions are considered in this study:

- (i) An equilibrium state is assumed reachable by fingertip rolling motion on the object surface.
- (ii) In the case of curved contact surfaces, fingertip motion is confined on a curvature of constant radius.
- (iii) The pressure distribution in the deformed area of each fingertip may be represented by a concentrated force at the center point of the contact area in the direction perpendicular to the object surface.
- (iv) Both fingertips are made of the same material.
- (v) The mass of the object is small enough to ignore the gravity effect.

Assumption (i) means that the initial state of the system does not necessarily correspond to an equilibrium. Assumption (ii) may be easily satisfied in practice as changes in contact positions by rolling fingertips are constrained by the tips' radius and the finger kinematics.

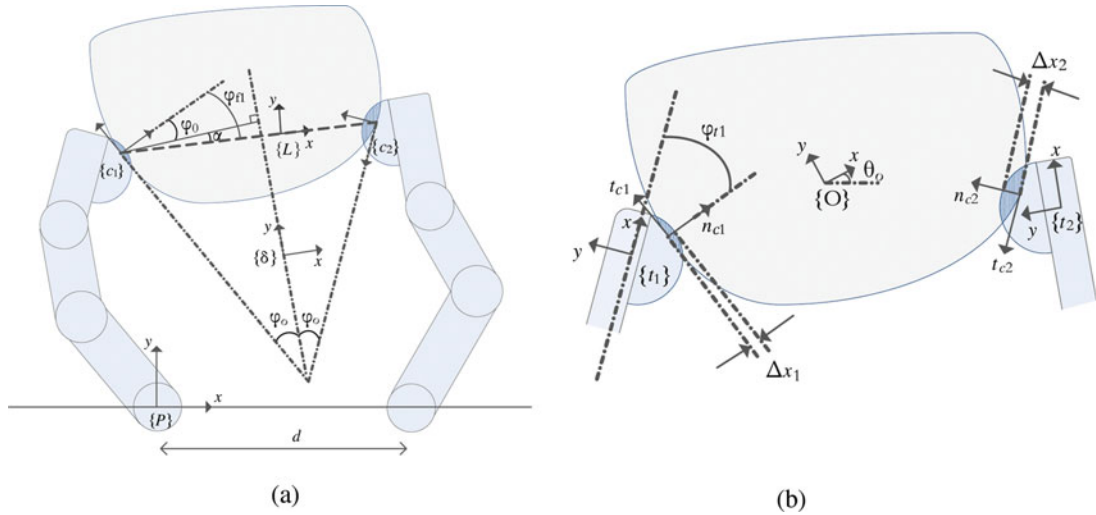


Fig. 1. (a) Pair of robotic fingers grasping a rigid arbitrary shaped object, (b) Object and finger tip frames.

Vector $\mathbf{q}_i = [q_{i1} \ q_{i2} \ q_{i3}]^T$, $i = 1, 2$ denotes the joint angles for the i th finger. In the following, R_{ab} denotes the rotation matrix of frame $\{b\}$ with reference to frame $\{a\}$ unless the reference frame is the inertia frame $\{P\}$ in which case it is omitted. Moreover, $R(\theta)$ is a rotation through an angle θ about the z axis that is normal to the x - y plane pointing outwards.

Let $\{P\}$ be the inertia frame attached at the base of the first finger (Fig. 1a) and $\{O\}$ be the object frame placed at its center of mass (Fig. 1b) and described by the position vector $\mathbf{p}_o \in \mathbb{R}^2$ and the rotation matrix $R_o = R(\theta_o)$. Let $\{t_i\}$ be the i th fingertip frame described by position vector $\mathbf{p}_{t_i} \in \mathbb{R}^2$ and rotation matrix $R_{t_i} = R(\phi_i)$, with $\phi_i = \sum_{j=1}^3 q_{ij}$.

Let the contact point of each finger be defined at the geometrical center of the contact area and be associated with a frame $\{c_i\}$ with its x axis aligned with the normal to the object surface pointing inwards. Let the orientation of $\{c_i\}$ relative to $\{t_i\}$ be described by $R_{t_i c_i} = R(\phi_{t_i})$ (Fig. 1b). Frame $\{c_i\}$ is described by position vector $\mathbf{p}_{c_i} \in \mathbb{R}^2$ and rotation matrix $R_{c_i} = R(\phi_i + \phi_{t_i})$. Let \mathbf{n}_{c_i} , $\mathbf{t}_{c_i} \in \mathbb{R}^2$ be the normal pointing inwards and the tangential vectors to the object at the contact points, expressed in $\{P\}$, hence $R_{c_i} = [\mathbf{n}_{c_i} \ \mathbf{t}_{c_i}]$. Notice that

$$\mathbf{p}_{c_i} = \mathbf{p}_{t_i} + (r - \Delta x_i)\mathbf{n}_{c_i}, \tag{1}$$

where Δx_i denotes the displacement due to the material deformation of each soft fingertip at the center of the contact area.

Let the two tangential lines at the contact points form an angle equal to $2\phi_0$ and $\{\delta\}$ be a frame with its y axis placed upon the bisector of the angle $2\phi_0$ at a position that can be freely chosen (Fig. 1a). Line c_1c_2 is the contact interaction line with length $\|\mathbf{p}_{c_2} - \mathbf{p}_{c_1}\| = l$ generally changing with the contact location for an arbitrary shaped object. Let $\{L\}$ be a frame with its x axis placed upon the interaction line c_1c_2 . The orientation of $\{L\}$ relative to $\{\delta\}$ is described by $R_{\delta L} = R(\alpha)$ (Fig. 1a). From the problem's geometry, it is clear that $R_{c_1 \delta} = R(\phi_0)$, $R_{c_2 \delta} = R(-\phi_0 - \pi)$. Combining the above $R_{c_1 L} = R(\phi_{f_1})$ and $R_{c_2 L} = R(\phi_{f_2} - \pi)$ where

$$\phi_{f_1} = \alpha + \phi_0, \ \phi_{f_2} = \alpha - \phi_0 \tag{2}$$

denote the angles between the interaction line and the normals to the contacts (Fig. 1a). Calculating the relative orientation of the contact frames $R_{c_1 c_2}$ via the object $R_{c_1 \delta} R_{c_2 \delta}^T$ and the fingers $R_{c_1}^T R_{c_2}$, angles ϕ_0 , ϕ_i , ϕ_{t_i} are related as follows:

$$2\phi_0 + \pi = \phi_2 - \phi_1 + \phi_{t_2} - \phi_{t_1} \tag{3}$$

We model the system under the following rolling constraints:⁷

$$\begin{bmatrix} A_{ii} & A_{i3} \end{bmatrix} \begin{bmatrix} \dot{\mathbf{q}}_i \\ \dot{\mathbf{p}}_o \\ \dot{\theta}_o \end{bmatrix} = 0, \tag{4}$$

where

$$A_{ii} = \mathbf{t}_{c_i}^T J_{v_i} + (r - \Delta x_i) J_{\omega_i}, \quad A_{i3} = \begin{bmatrix} -\mathbf{t}_{c_i}^T & \mathbf{t}_{c_i}^T \hat{\mathbf{p}}_{oc_i} \end{bmatrix} \tag{5}$$

with $\mathbf{p}_{oc_i} = \mathbf{p}_{c_i} - \mathbf{p}_o$ and for a vector $\mathbf{p} = [a \ b]^T$ we define $\hat{\mathbf{p}} = [-b \ a]^T$ so that $\forall \mathbf{k} \in \mathbb{R}^2$, $\hat{\mathbf{p}}^T \mathbf{k}$ denotes the outer product $\mathbf{p} \times \mathbf{k}$. The Jacobian matrices $J_{v_i} = J_{v_i}(\mathbf{q}_i) \in \mathbb{R}^{2 \times 3}$, $J_{\omega_i} = J_{\omega_i}(\mathbf{q}_i) \in \mathbb{R}^{1 \times 3}$ relate the joint velocity $\dot{\mathbf{q}}_i \in \mathbb{R}^3$ with the i th fingertip linear and rotational velocities $\dot{\mathbf{p}}_{t_i} \in \mathbb{R}^2$ and $\omega_{t_i} = \dot{\phi}_i \in \mathbb{R}$, respectively as follows:

$$\dot{\mathbf{p}}_{t_i} = J_{v_i} \dot{\mathbf{q}}_i, \quad \omega_{t_i} = J_{\omega_i} \dot{\mathbf{q}}_i. \tag{6}$$

Given assumption (iii), we adopt the following model⁴² for the normal force magnitude:

$$f_i = k_i \Delta x_i^2 + \xi_i \Delta \dot{x}_i, \tag{7}$$

where k_i is a fingertip material-based parameter and ξ_i is the viscous friction damping coefficient of the elastic material. Given assumption (iv), $k_1 = k_2 = k$, $\xi_1 = \xi_2 = \xi$.

The system dynamics, under the rolling constraints (4) and assumption (v), is described by the following equations for both fingers and the object:

$$M_i(\mathbf{q}_i) \ddot{\mathbf{q}}_i + C_i(\mathbf{q}_i, \dot{\mathbf{q}}_i) \dot{\mathbf{q}}_i + D_{ii}^T f_i + A_{ii}^T \lambda_i = \mathbf{u}_i, \tag{8}$$

$$M \begin{bmatrix} \ddot{\mathbf{p}}_o \\ \ddot{\theta}_o \end{bmatrix} + D_{13}^T f_1 + D_{23}^T f_2 + A_{13}^T \lambda_1 + A_{23}^T \lambda_2 = 0, \tag{9}$$

where

$$D_{ii} = \mathbf{n}_{c_i}^T J_{v_i}, \quad D_{i3} = \begin{bmatrix} -\mathbf{n}_{c_i}^T & \mathbf{n}_{c_i}^T \hat{\mathbf{p}}_{oc_i} \end{bmatrix}, \tag{10}$$

$M_i(\mathbf{q}_i) \in \mathbb{R}^{3 \times 3}$, $M = \text{diag}(M_o, I_o)$, with $M_o = \text{diag}(m_o, m_o)$ the positive definite inertia matrices of the i th finger and object, respectively and m_o, I_o denote the object's mass and moment of inertia and $C_i(\mathbf{q}_i, \dot{\mathbf{q}}_i) \dot{\mathbf{q}}_i \in \mathbb{R}^3$ the vector of Coriolis and centripetal forces of the i th finger. The Lagrange multipliers λ_i represent the applied tangential constraint forces at the contacts and let f_{c_i} denote the resultant contact force magnitude. Last, $\mathbf{u}_i \in \mathbb{R}^3$ is the vector of applied joint torques to the i th finger.

3. Grasp and Finger Relative Orientation Control

The following grasping controller is proposed for achieving a stable grasp of an arbitrary-shaped object with soft fingertips:

$$\mathbf{u}_i = -k_{v_i} \dot{\mathbf{q}}_i - (-1)^i f_d J_{v_i}^T \frac{\mathbf{p}_{t_2} - \mathbf{p}_{t_1}}{\|\mathbf{p}_{t_2} - \mathbf{p}_{t_1}\|} - (-1)^i r f_d \sin \phi J_{\omega_i}^T, \tag{11}$$

where

$$\phi = \phi_2 - \phi_1 - \gamma_s, \tag{12}$$

k_{v_i}, f_d are positive constants and γ_s is an angle which is set by the designer in order to express the desired relative orientation of the two fingers. Hereafter, the following compact notation is used for an angle θ : $s_\theta \triangleq \sin \theta$ and $c_\theta \triangleq \cos \theta$.

The first term of Eq. (11) is introduced for joint damping. The second term represents applied forces of magnitude f_d at the direction of the line connecting the fingertips $\vec{t}_1\vec{t}_2 \triangleq \frac{\mathbf{p}_{t_2}-\mathbf{p}_{t_1}}{\|\mathbf{p}_{t_2}-\mathbf{p}_{t_1}\|}$ and the third term expresses the tangential contact forces at equilibrium as it will be clarified in the next section.

This controller was proved to achieve the control objective in the case of fingers with rigid tips.⁴¹ In this work, we prove (Section 5) that the proposed controller (11), (12) achieves the control objectives in the case of soft fingertips and hence it can be successfully utilized in either case.

Remark 1. The proposed control law (11) and (12) can be calculated using only the robotic finger forward kinematics and the undeformed radius of the hemispherical tips. It does not require any knowledge of the tangential and normal directions at the contact, unlike Song et al. [34], and therefore no tactile sensing is needed. Moreover, in contrast with other previous work,³⁹ it does not require the use of on line estimates of tangential forces, neither conditions the grasping force magnitude on system parameters.

Remark 2. The accommodation of additional objectives to the grasp stability is made possible by the system’s redundancy. In fact, the system consisted of the two soft-tipped fingers and the object has seven DOF to satisfy the control objectives: four DOF for stable grasping and one DOF for the desired relative finger orientation leaving two DOF free for other control objectives.

4. System Equilibrium

Substituting (11) into (8) utilizing (10) and (4) expanded by (5), the closed loop system can be written in terms of the force errors as follows:

$$M_i \ddot{\mathbf{q}}_i + C_{f_i} \dot{\mathbf{q}}_i + D_{ii}^T \Delta f_i + A_{ii}^T \Delta \lambda_i + J_{\omega_i}^T \Delta N_i = 0, \tag{13}$$

$$M_o \ddot{\mathbf{p}}_o - \sum_{i=1}^2 (\mathbf{n}_{c_i} \Delta f_i + \mathbf{t}_{c_i} \Delta \lambda_i) = 0, \tag{14}$$

$$I_o \ddot{\theta}_o + \sum_{i=1}^2 \hat{\mathbf{p}}_{oc_i}^T (\mathbf{n}_{c_i} \Delta f_i + \mathbf{t}_{c_i} \Delta \lambda_i) + S_N = 0, \tag{15}$$

where

$$\Delta f_i = f_i - (-1)^{i+1} f_d \mathbf{n}_{c_i}^T \vec{t}_1\vec{t}_2, \tag{16}$$

$$\Delta \lambda_i = \lambda_i - (-1)^{i+1} f_d \mathbf{t}_{c_i}^T \vec{t}_1\vec{t}_2, \tag{17}$$

$$\Delta N_i = (-1)^{i+1} f_d \left((r - \Delta x_i) \mathbf{t}_{c_i}^T \vec{t}_1\vec{t}_2 - r s_\phi \right), \tag{18}$$

$$S_N = (\hat{\mathbf{p}}_{oc_1}^T - \hat{\mathbf{p}}_{oc_2}^T) f_d \vec{t}_1\vec{t}_2, \tag{19}$$

and $C_{f_i} = (C_i + k_{v_i} I_3)$ with I_3 being the identity matrix of dimension 3.

The system equilibrium is found by setting velocities and accelerations to zero in Eqs. (13)–(15). From Eqs. (14) and (15), it is easy to derive that $S_N = 0$ and in turn utilizing Eq. (19)

$$(\hat{\mathbf{p}}_{oc_2}^T - \hat{\mathbf{p}}_{oc_1}^T) \vec{t}_1\vec{t}_2 = 0. \tag{20}$$

Notice that $\mathbf{p}_{oc_2} - \mathbf{p}_{oc_1} = \mathbf{p}_{c_2} - \mathbf{p}_{c_1} \triangleq c_1\vec{c}_2$ is the interaction line vector; hence, Eq. (20) indicates a zero outer product of $c_1\vec{c}_2, \vec{t}_1\vec{t}_2$ which implies that these lines are parallel at equilibrium. Also, Eq. (13) yields $D_{ii}^T \Delta f_i + A_{ii}^T \Delta \lambda_i + J_{\omega_i}^T \Delta N_i = 0$ which using Eq. (10), Eq. (5) can be written as

$[J_{v_i}^T \ J_{\omega_i}^T] \begin{bmatrix} \mathbf{n}_{ci} \Delta f_i + \mathbf{t}_{ci} \Delta \lambda_i \\ r(\Delta \lambda_i + \Delta N_i) \end{bmatrix} = 0$. Assuming a full rank Jacobian matrix $J_i = [J_{v_i}^T \ J_{\omega_i}^T]$, we obtain $\mathbf{n}_{ci} \Delta f_i + \mathbf{t}_{ci} \Delta \lambda_i = 0$, $\Delta \lambda_i + \Delta N_i = 0$ and owing to the independent directions:

$$\Delta f_i = \Delta \lambda_i = 0, \tag{21}$$

$$\Delta N_i = 0. \tag{22}$$

Consequently, since $\vec{t_1 t_2}$ is parallel to $\vec{c_1 c_2}$, force angles at equilibrium satisfy the following:

$$\tan^{-1} \left(\frac{\lambda_i}{f_i} \right) = \phi_{f_i}. \tag{23}$$

Also, contact forces lie on the interaction line with magnitude $f_{c_i} = f_d$. Alternatively from Eq. (21), utilizing Eq. (7) yields

$$\Delta x_i^2 = \frac{f_d}{k} \cos \phi_{f_i}. \tag{24}$$

Subtracting Eq. (24) for $i = 1, 2$ and using Eq. (2) yields

$$\Delta x_1^2 - \Delta x_2^2 = -\frac{2f_d}{k} s_\alpha s_{\phi_0}, \tag{25}$$

which means that when both fingers apply the same normal contact forces at equilibrium ($\Delta x_1 = \Delta x_2$), then $\alpha = 0$ (or $\phi_0 = 0$) and vice versa.

Moreover, from Eq. (18) owing to Eq. (22), it is proved that at equilibrium

$$s_\phi = \frac{r - \Delta x_i}{r} \mathbf{t}_{ci}^T \vec{t_1 t_2}, \tag{26}$$

which yields for the relative fingertip orientation:

$$\phi_2 - \phi_1 = \beta + \gamma_s, \tag{27}$$

where

$$\sin \beta = \frac{r - \Delta x_i}{r} \sin \left(\phi_0 + (-1)^{i+1} \alpha \right). \tag{28}$$

From Eq. (27), the way γ_s affects the final relative finger orientation is made clear. Equation (28) for relative stiff materials ($\frac{r - \Delta x_i}{r} \approx 1$) yields

$$\beta = \phi_0 + (-1)^{i+1} \alpha, \tag{29}$$

which implies that $\alpha = 0$ and hence $\beta = \phi_0$. Then, Eq. (2) implies that $\phi_{f_1} = -\phi_{f_2} = \phi_0$ which is the best compromise achieved for stable grasping since both finger contact forces are equally placed within the friction cone. This is also generally true as it is shown in simulation results. Moreover, when $\alpha = 0$, the bisector of $2\phi_0$ is perpendicular to the interaction line at equilibrium.

Remark 3. Given $\alpha = 0$, Eq. (27) indicates that for objects with parallel surfaces ($\phi_0 = 0$) or known ϕ_0 , γ_s specifies accurately the relative fingertip orientation at equilibrium.

Summarizing the equilibrium state manifold of the closed loop system:

- Fingertip line $\vec{t_1 t_2}$ is parallel to the interaction line $\vec{c_1 c_2}$.
- Contact forces $[f_i \ \lambda_i]^T$ applied along $\vec{t_1 t_2}$ direction have a magnitude $f_{c_i} = f_d$.
- The final relative finger orientation is $\phi_2 - \phi_1 = \beta + \gamma_s$.

5. Stability Analysis

To facilitate the analysis, we rewrite the closed loop system Eqs. (8)–(11) in the following compact form collecting all Lagrange multipliers in the vector $\lambda = [\lambda_1 \ \lambda_2]^T$ and all system position variables in $\mathbf{x} = [\mathbf{q}_1^T \ \mathbf{q}_2^T \ \mathbf{p}_o^T \ \theta_o]^T$.

$$M_s \ddot{\mathbf{x}} + C_s \dot{\mathbf{x}} + K_v \dot{\mathbf{x}} + D \mathbf{f} + A \lambda - f_d \begin{bmatrix} J_{v_1}^T \vec{t}_1 \vec{t}_2 \\ -J_{v_2}^T \vec{t}_1 \vec{t}_2 \\ 0_{3 \times 1} \end{bmatrix} - f_d \begin{bmatrix} J_{\omega_1}^T r s_\phi \\ -J_{\omega_2}^T r s_\phi \\ 0_{3 \times 1} \end{bmatrix} = 0 \tag{30}$$

with

$$\begin{aligned} M_s &= \text{diag}(M_1, M_2, M) \quad , \quad C_s = \text{diag}(C_1, C_2, 0_{3 \times 3}), \\ K_v &= \text{diag}(k_{v_1} I_3, k_{v_2} I_3, 0_{3 \times 3}) \quad , \quad \mathbf{f} = [f_1 \ f_2]^T, \\ A &= \begin{bmatrix} A_{11}^T & 0_{3 \times 1} \\ 0_{3 \times 1} & A_{22}^T \\ A_{13}^T & A_{23}^T \end{bmatrix} \quad , \quad D = \begin{bmatrix} D_{11}^T & 0_{3 \times 1} \\ 0_{3 \times 1} & D_{22}^T \\ D_{13}^T & D_{23}^T \end{bmatrix}. \end{aligned} \tag{31}$$

Similarly, the constraints can be written compactly as $A^T \dot{\mathbf{x}} = 0$.

Multiplying Eq. (30) by $\dot{\mathbf{x}}^T$ from the left and considering a constant desired relative fingertip orientation ($\dot{\gamma}_s = 0$) yields $\frac{dV}{dt} + W = 0$, where

$$V = \frac{1}{2} \dot{\mathbf{x}}^T M_s \dot{\mathbf{x}} + f_d \|\mathbf{p}_{t_1} - \mathbf{p}_{t_2}\| + f_d r z(t) + \sum_{i=1}^2 b_i(t), \tag{32}$$

$$W = \sum_{i=1}^2 \left(k_{v_i} \|\dot{\mathbf{q}}_i\|^2 + \xi_i \Delta \dot{x}_i^2 \right) \tag{33}$$

with $z(t) = \int_0^\phi s_\xi d\xi$, $b_i(t) = \int_0^{\Delta x_i} f_s(\zeta) d\zeta$, and $f_s(\Delta x_i) = k_i \Delta x_i^2$. Clearly, V is positive definite with respect to $\dot{\mathbf{x}}$, $\|\mathbf{p}_{t_1} - \mathbf{p}_{t_2}\|$, $z(t)$ for $-\frac{\pi}{2} < \phi < \frac{\pi}{2}$ and $b_i(t)$ for $0 < \Delta x_i < r$ in the constraint manifold defined by $\mathcal{M}_c(\mathbf{x}) = \{\mathbf{x} \in \mathbb{R}^9 : A^T \dot{\mathbf{x}} = 0\}$. It is clear that $V(t) \leq V(0)$ holds and consequently $\dot{\mathbf{x}}$, $\|\mathbf{p}_{t_1} - \mathbf{p}_{t_2}\|$, $z(t)$, and $b_i(t)$ are bounded. The time derivation of Eq. (1) yields $\Delta \dot{x}_i = \mathbf{n}_{c_i}^T (\dot{\mathbf{p}}_{t_i} - \dot{\mathbf{p}}_{c_i})$. Hence, $\Delta \dot{x}_i$ is bounded. From Eqs. (16), (18)–(19) using Eq. (7), it can easily be concluded that Δf_i , ΔN_i , and S_N are also bounded.

We write alternatively the closed loop system (13)–(15) in the following form utilizing Eqs. (10) and (5):

$$M_s \ddot{\mathbf{x}} + C \dot{\mathbf{x}} + D \Delta \mathbf{f} + A \Delta \lambda + B \Delta \mathbf{m} = 0, \tag{34}$$

$$\begin{aligned} C &= C_s + K_v \quad , \quad B = \begin{bmatrix} r J_{\omega_1}^T & 0_{3 \times 1} & 0_{3 \times 1} \\ 0_{3 \times 1} & r J_{\omega_2}^T & 0_{3 \times 1} \\ 0_{3 \times 1} & 0_{3 \times 1} & [0 \ 0 \ 1]^T \end{bmatrix} \\ \Delta \mathbf{f} &= [\Delta f_1 \ \Delta f_2]^T, \quad \Delta \lambda = [\Delta \lambda_1 \ \Delta \lambda_2]^T, \quad \Delta \mathbf{m} = [\Delta N_1 \ \Delta N_2 \ S_N]^T. \end{aligned} \tag{35}$$

In order to prove that $\Delta \lambda$ is bounded, we multiply Eq. (34) by $A^T M_s^{-1}$ from the left, substituting $A^T \ddot{\mathbf{x}} = -\dot{A}^T \dot{\mathbf{x}}$ and multiplying again by $(A^T M_s^{-1} A)^{-1}$, we derive

$$\Delta \lambda = (A^T M_s^{-1} A)^{-1} (\dot{A}^T \dot{\mathbf{x}} - A^T M_s^{-1} (C \dot{\mathbf{x}} + D \Delta \mathbf{f} + B \Delta \mathbf{m})).$$

Since Δf_i , ΔN_i , and S_N are bounded, $\Delta \mathbf{f}$ and $\Delta \mathbf{m}$ are bounded and hence the term in the second parenthesis is bounded. Additionally, the matrix in the first parenthesis is bounded, thus $\Delta \lambda$ is

bounded. Hence from Eq. (34), $\ddot{\mathbf{x}}$ is also bounded and consequently $\dot{\mathbf{x}}$ is uniformly continuous. We may therefore deduce the convergence of \mathbf{q}_i to zero while the rolling constrains (4) yield that

$$\dot{\mathbf{p}}_o - \hat{p}_{oci} \dot{\theta}_o \rightarrow 0. \tag{36}$$

Eliminating $\dot{\mathbf{p}}_o$ by subtracting Eq. (36) (for $i = 1, 2$) yields $(\hat{p}_{oc2} - \hat{p}_{oc1}) \dot{\theta}_o \rightarrow 0$ and in turn $\dot{\theta}_o \rightarrow 0$ and from Eq. (36), $\dot{\mathbf{p}}_o \rightarrow 0$. Hence, it is proved that system velocities converge to zero, $\dot{\mathbf{x}} \rightarrow 0$. Following the reasoning of Section 4, we obtain $\Delta f_i, \Delta \lambda_i, \Delta N_i \rightarrow 0$. Since $\dot{\mathbf{x}}$ is bounded, \mathbf{x} is uniformly continuous, therefore $\Delta \mathbf{f}, \Delta \boldsymbol{\lambda}$, and $\Delta \mathbf{m}$ are uniformly continuous from Eqs. (16) and (17). Consequently, Eq. (34) leads to $\ddot{\mathbf{x}}$ being uniformly continuous, thus $\ddot{\mathbf{x}} \rightarrow 0$. Last from the rotational object Eq. (15), it is clear that $S_N \rightarrow 0$. Regarding \mathbf{x} convergence, it may be further proved following the proof line in Arimoto³⁶ that $\dot{\mathbf{x}}$ converges to zero exponentially as $t \rightarrow \infty$.

6. Simulation Results

We consider two identical robotic fingers, as depicted in Fig. 1a, with $r = 0.01$ m and their parameters given in Table I. The fingers are positioned at distance $d = 0.02$ m and are initially at rest while applying a normal contact force of 2 N. The fingertip material parameters are chosen as $k = 5 \times 10^4$ Nm^{-2} and $\xi = 3$ Nm^{-1}s .

We consider three types of objects, an object with parallel surfaces ($\phi_0 = 0^\circ$), a trapezoidal object ($\phi_0 = -12.5^\circ$) and an object with a curved surface of semicircular shape (varying ϕ_0). The parameters of the objects are given in Table II. The system is simulated under the proposed controller with $k_{v_i} = 0.005$ Nm/s for $i = 1, 2$ and $f_d = 4$ N. The initial relative orientation of the fingers is chosen as $\phi_2(0) - \phi_1(0) = 95^\circ$ and the object is initially at $\theta_o = 0^\circ$.

Table I. Robotic fingers parameters.

Links	1	2	3
Masses (Kg)	0.045	0.03	0.015
Lengths (m)	0.04	0.03	0.02
Inertias (Kg m ²) $I_z (\times 10^{-6})$	6	4	2

Table II. Parameters of the grasped objects.

Object with parallel surfaces	
Mass (kg)	0.04
Height (m)	0.04
Width (m)	0.02
Trapezoidal object	
Mass (kg)	0.04
Height (m)	0.05
Small base (m)	0.02
Side angles (°)	15 and 10
Curved object	
Mass (kg)	0.04
Radius (m)	0.02

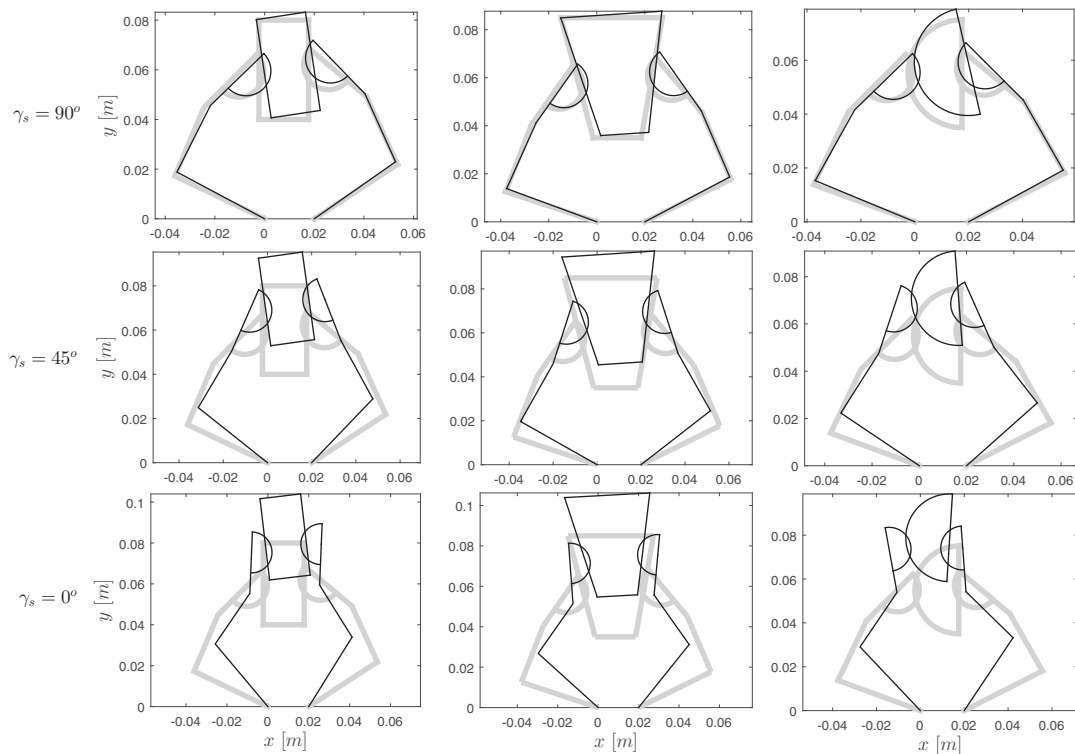


Fig. 2. System equilibrium for $\gamma_s = 90^\circ$, $\gamma_s = 45^\circ$, and $\gamma_s = 0^\circ$ for all object shapes (the gray line represents the initial and the black line the equilibrium system configuration).

Figure 2 shows the initial and equilibrium system configuration for all object shapes and for three different desired relative finger orientations $\gamma_s = 90^\circ$, $\gamma_s = 45^\circ$, and $\gamma_s = 0^\circ$. A desired $\gamma_s = 90^\circ$ keeps close to the initial configuration which is useful if grasp preshapes should be preserved while with $\gamma_s = 0^\circ$ the distal links are almost parallel to each other. Moreover, Fig. 3 shows the internal force manipulability ellipsoids^{43–45} at the equilibrium system configuration for all object shapes and desired relative finger orientations. Internal force manipulability ellipsoids are defined by regarding the whole cooperative system as a mechanical transformer from the joint space to the cooperative task space. It is clear that the relative finger orientation with $\gamma_s = 90^\circ$ is appropriate when larger grasping forces are required (bulky object) as opposed to $\gamma_s = 0^\circ$ which is more suitable for delicate tip forces (thin object).³ Figure 4 shows that angle α goes to zero for all desired finger relative orientations and object shapes, achieving the best compromise regarding force angles as mentioned in Section 4.

System time response is shown for the case of the object with a curved surface and $\gamma_s = 0^\circ$ in Figs. 5–11 and is consistent with theoretical findings. Joint and object velocities as well as force and torque errors converge to zero (Figs. 5a, 5b–6, respectively). Fingertip line t_1t_2 is parallel to the interaction line c_1c_2 at equilibrium (Fig. 7) and the resulting grasping force f_{c_i} (Fig. 8) is converging to the desired magnitude $f_d = 4$ N. The evolution of angles α and ϕ_0 is shown in Fig. 9a where it is clear that ϕ_0 is changing in this case and angle α is converging to zero. This means that the force angles (2) are converging to ϕ_0 (Fig. 10) while staying less than 20° during grasping. This also means that both fingers are applying the same amount of normal contact forces as it is shown by the fingertip deformations in Fig. 11. Finally, angle ϕ converges to the value of β for $i = 1, 2$ (Fig. 9b) satisfying the equilibrium relation (27).

Last, we demonstrate the use of the γ_s control parameter in achieving a transfer from one fingertip relative orientation to another without compromising stability. This could be useful for cases where the subsequent task of the robot benefits from a different relative finger orientation. If, for example,

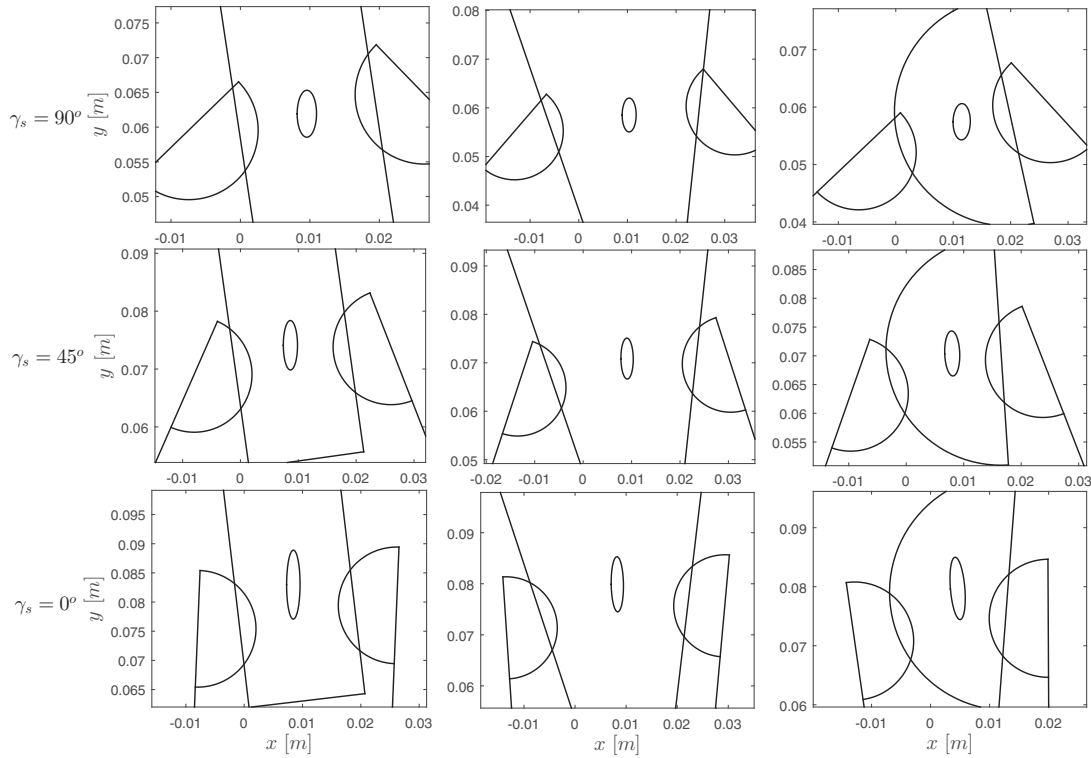


Fig. 3. Internal force manipulability ellipsoids (scaled by 0.03%) for $\gamma_s = 90^\circ$, $\gamma_s = 45^\circ$, and $\gamma_s = 0^\circ$ for all object shapes.

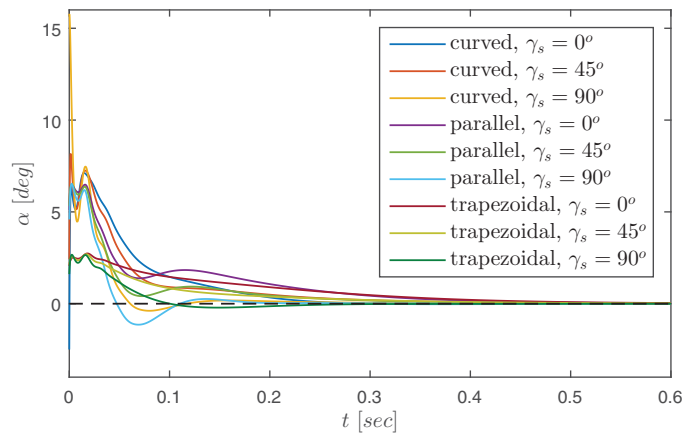


Fig. 4. Angle α for all cases.

the grasped object should be placed in a narrow or clustered environment, $\gamma_s = 0^\circ$ would provide a more compact finger-object cluster as compared to $\gamma_s = 90^\circ$ (Fig. 2). In the following simulation results, after achieving a stable grasp with $\gamma_s = 90^\circ$, we transition to $\gamma_s = 0^\circ$ via $\gamma_s(t) = \frac{\pi}{2}e^{-10t}$ at $t = 2$ s for the object with a curved surface. Figure 12 shows the system pose when the object is stably grasped with $\gamma_s = 90^\circ$ as well as the final system pose with $\gamma_s = 0^\circ$. Finally, Figs. 13–14 show that

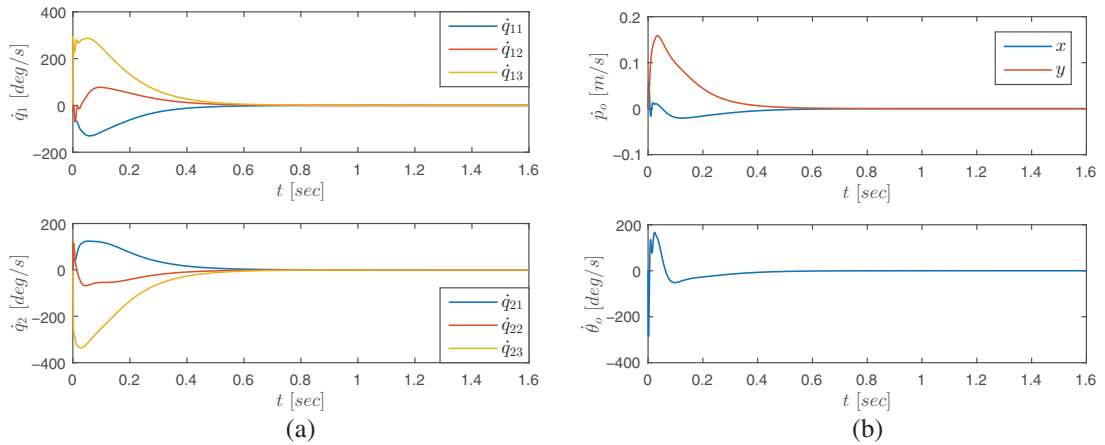


Fig. 5. (a) Joint angular velocities, (b) Object translational and angular velocities.

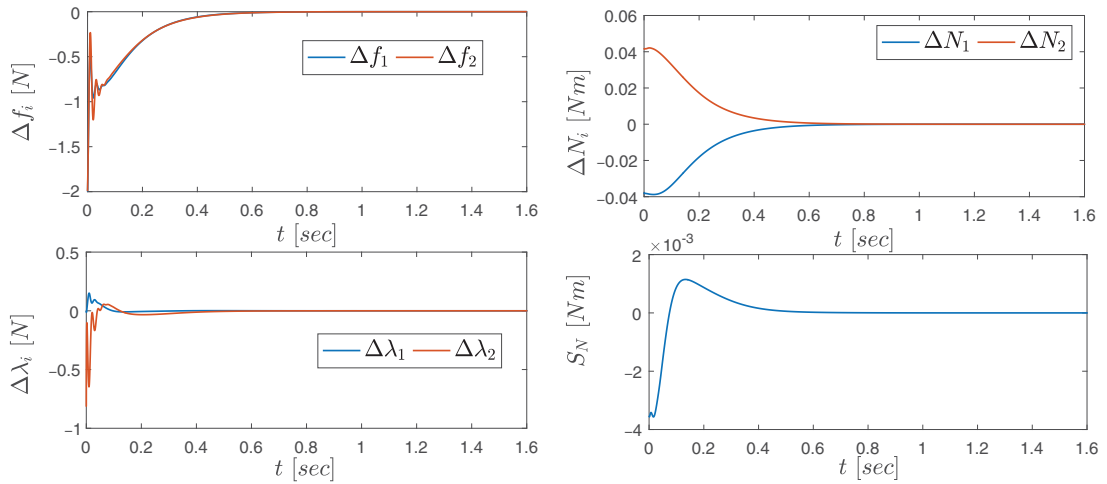


Fig. 6. Responses of (a) Normal force error Δf_i . (b) Tangential force error $\Delta \lambda_i$. (c) Finger torque error ΔN_i . (d) Object torque error S_N .

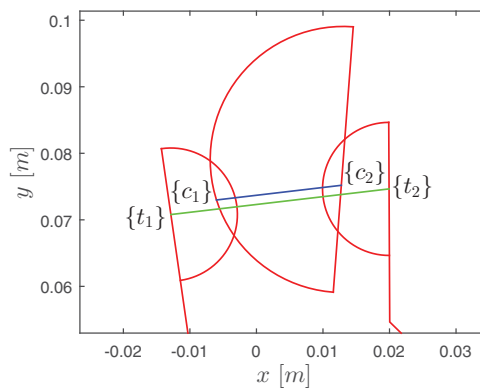


Fig. 7. Fingertip and interaction lines at equilibrium.

all velocities and errors converge to zero at the end of the transition while the force angles stay less than 25° during all stages (Fig. 15). Angle α converges to zero and angle ϕ converges to the values of β (Fig. 16). It is clear that the stability of the system is not compromised.

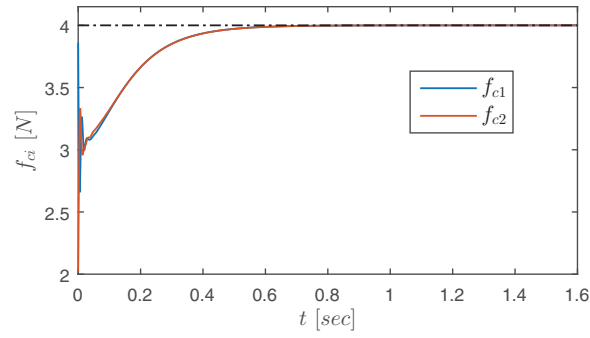


Fig. 8. Grasping force response.

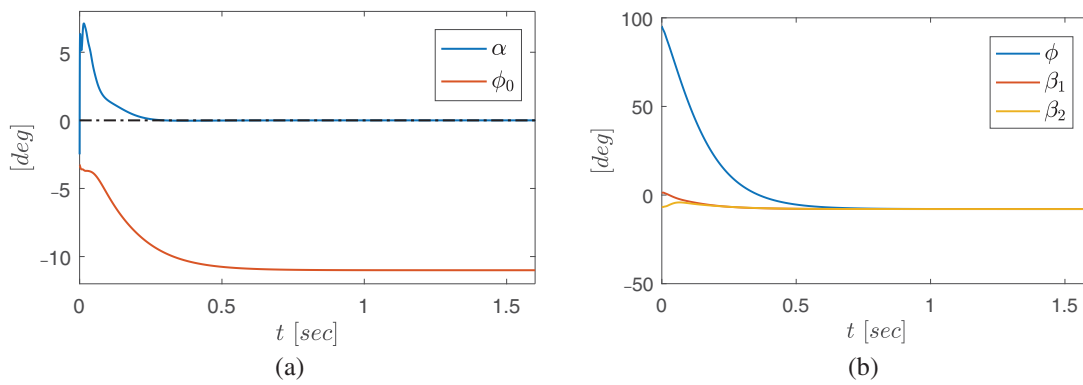


Fig. 9. (a) Angles α and ϕ_0 , (b) Angles ϕ and β_i .

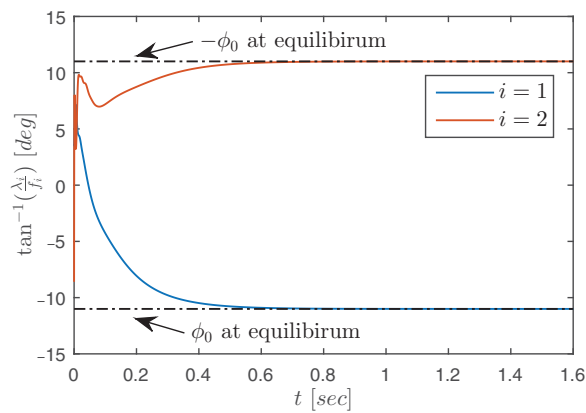


Fig. 10. Force angles.

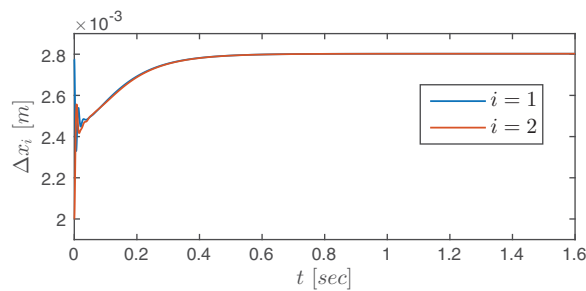


Fig. 11. Fingertip deformation.

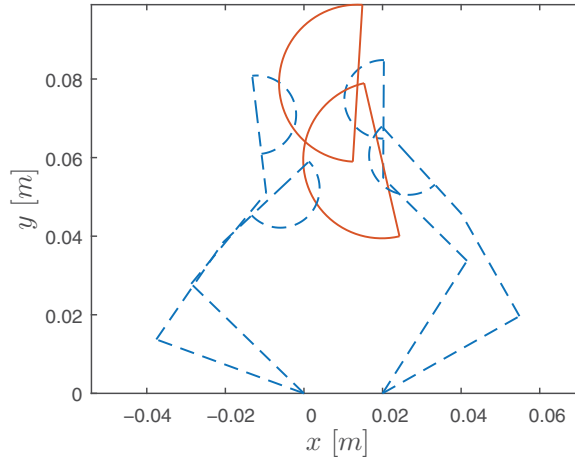


Fig. 12. Transition from a stable grasp with $\gamma_s = 90^\circ$ to a stable grasp with $\gamma_s = 0^\circ$.

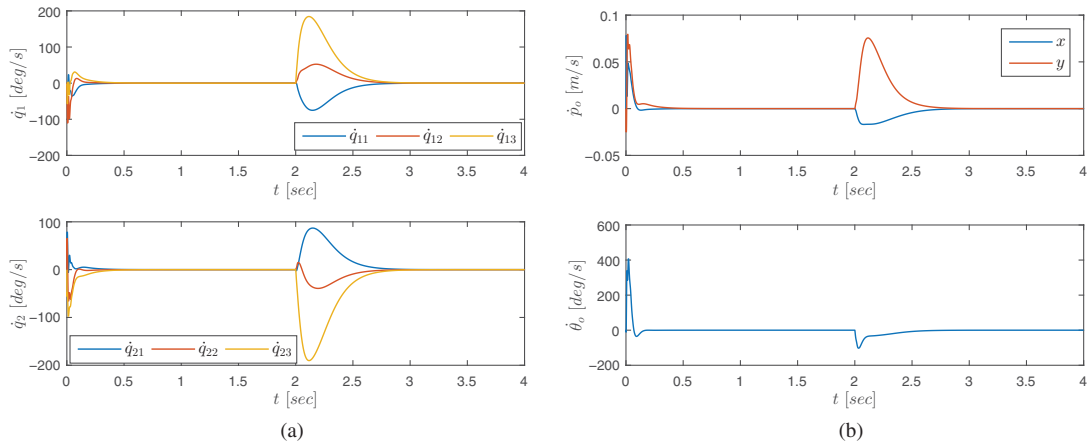


Fig. 13. (a) Joint angular velocities, (b) Object translational and angular velocities during transition from a stable grasp with $\gamma_s = 90^\circ$ to a stable grasp with $\gamma_s = 0^\circ$.

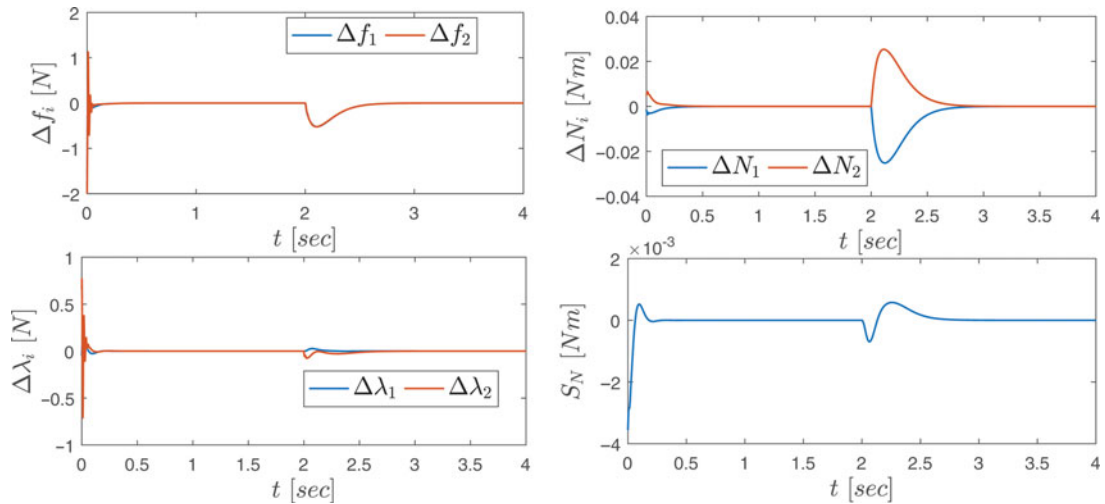


Fig. 14. Responses of (a) Normal force error Δf_i . (b) Tangential force error $\Delta \lambda_i$. (c) Finger torque error ΔN_i . (d) Object torque error S_N during transition from a stable grasp with $\gamma_s = 90^\circ$ to a stable grasp with $\gamma_s = 0^\circ$.

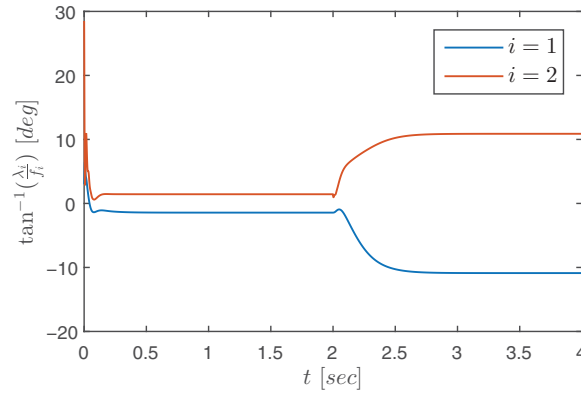


Fig. 15. Force angles during transition from a stable grasp with $\gamma_s = 90^\circ$ to a stable grasp with $\gamma_s = 0^\circ$.

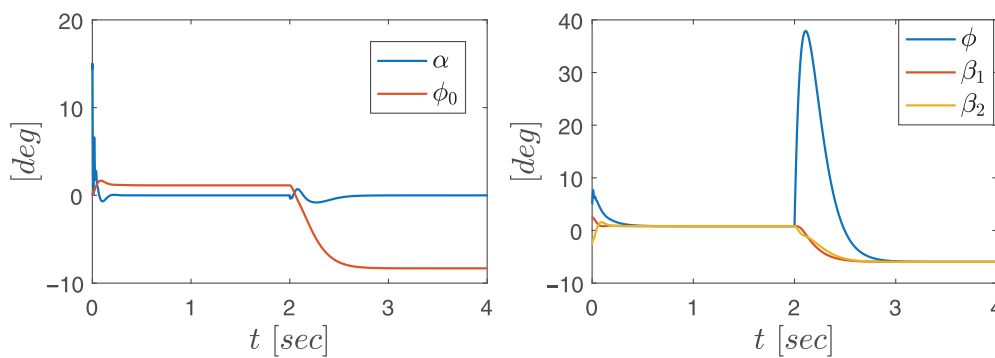


Fig. 16. Angles α , ϕ_0 , ϕ and β_i during transition from a stable grasp with $\gamma_s = 90^\circ$ to a stable grasp with $\gamma_s = 0^\circ$.

7. Experimental Results

We further validate the proposed controller via experimental results. The experiments were conducted using a prototype robotic hand setup developed in the Human-Centered Robotics Laboratory of Kyushu University in Fukuoka, Japan (Fig. 17) by Tahara *et al.* [46]. The robotic hand consists of three four-DOF fingers, only two of which were used for this experimental validation. The joint structure of the fingers is shown in Fig. 18 and their parameters are given in Table III. The hemispherical fingertips are made of silicon and their radius is $r = 0.015$ m. The actuators used in the configuration



Fig. 17. The prototype robotic hand setup.

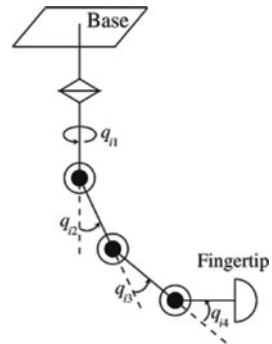
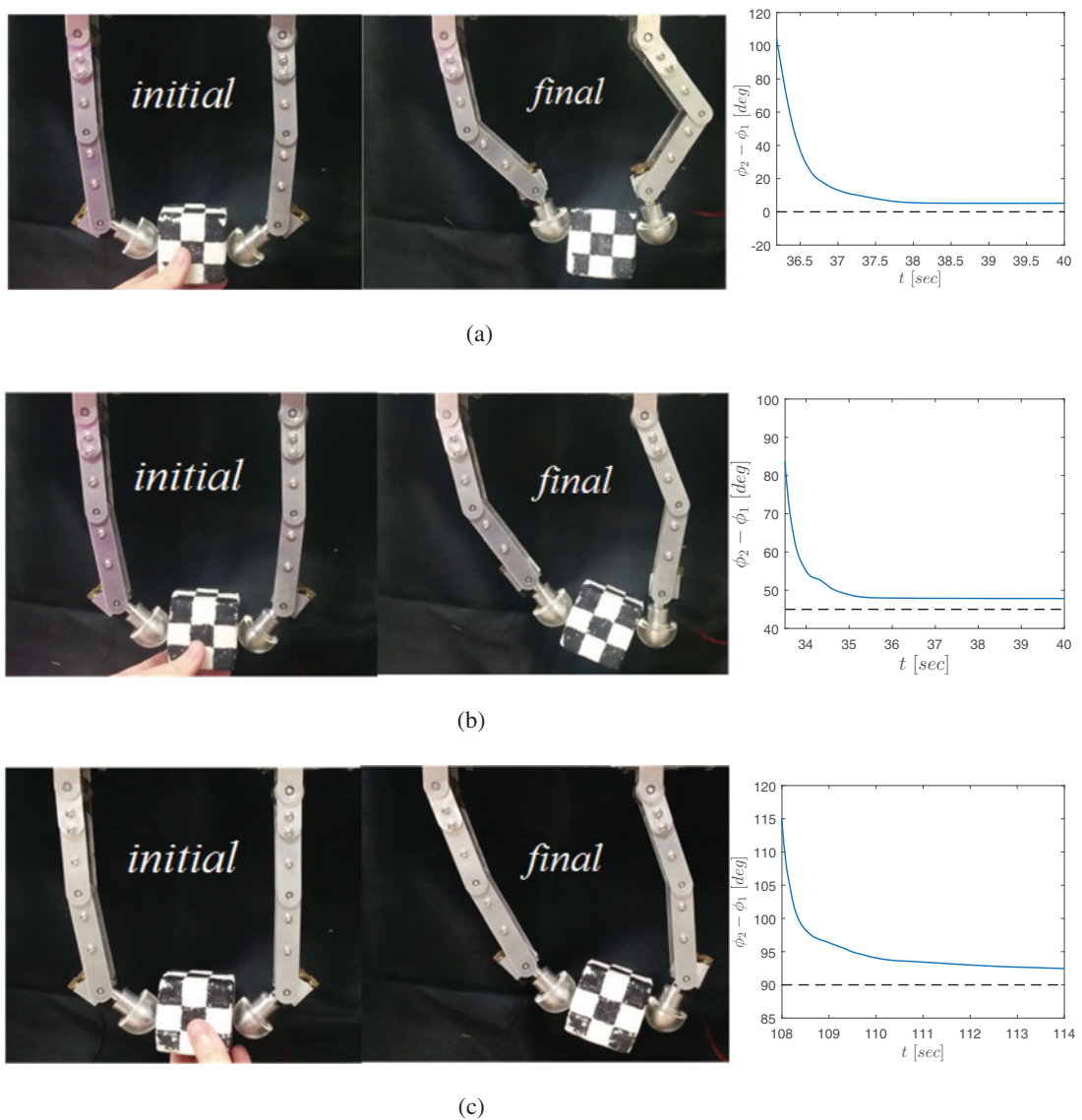


Fig. 18. Joint structure of the prototype robotic fingers.

Fig. 19. Stable grasping of a cube with different γ_s (the dashed line corresponds to γ_s and the solid line to the relative finger orientation $\phi_2 - \phi_1$). (a) $\gamma_s = 0^\circ$. (b) $\gamma_s = 45^\circ$. (c) $\gamma_s = 90^\circ$.

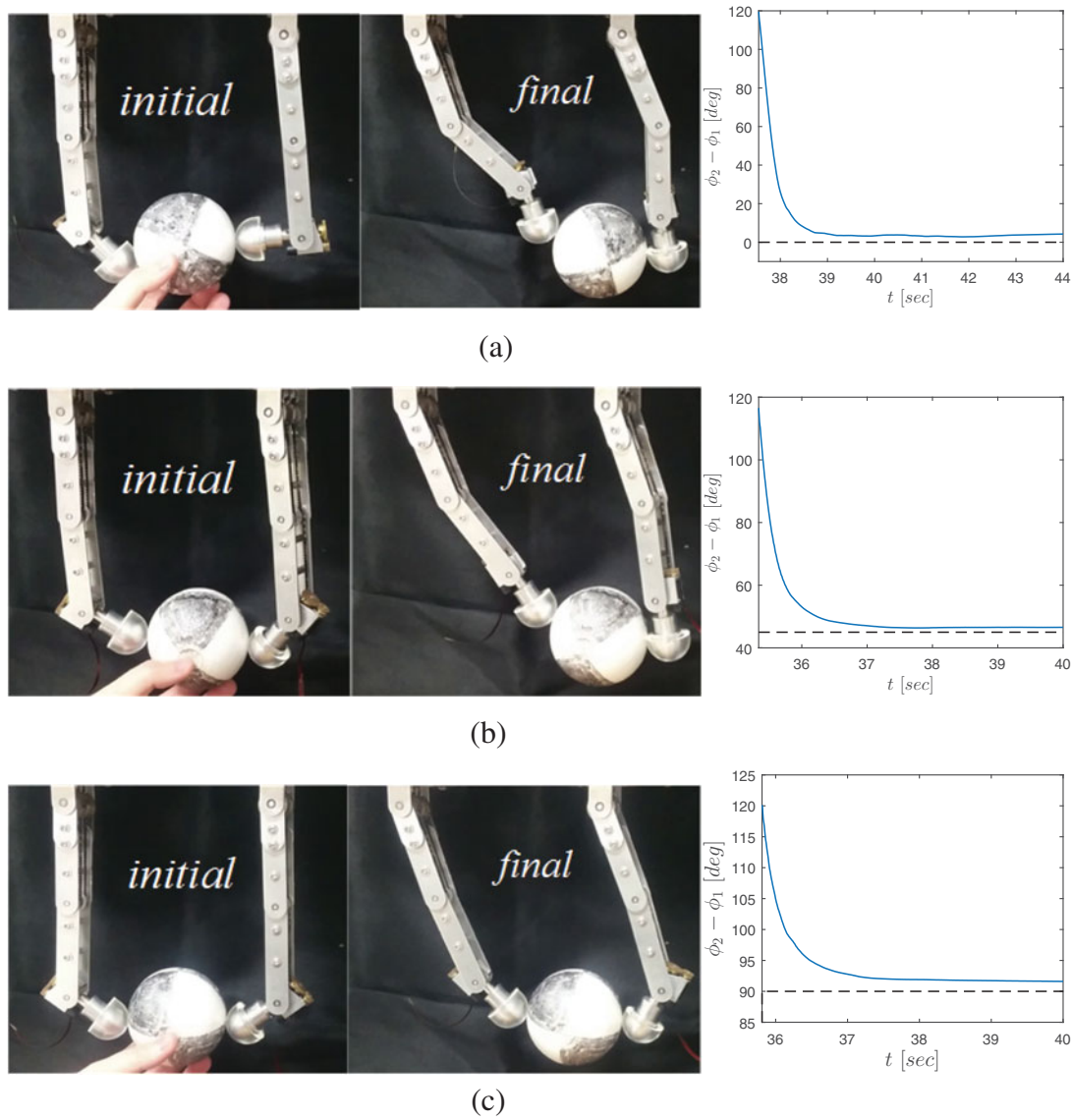


Fig. 20. Stable grasping of a sphere with different γ_s (the dashed line corresponds to γ_s and the solid line to the relative finger orientation $\phi_2 - \phi_1$). (a) $\gamma_s = 0^\circ$. (b) $\gamma_s = 45^\circ$. (c) $\gamma_s = 90^\circ$.

Table III. The prototype robotic fingers parameters.

Links	1	2	3
Masses (Kg)	0.038	0.024	0.054
Lengths (m)	0.064	0.064	0.03
Mass center (m)	0.023	0.035	0.01

are DC motors with specifications given in Table IV. The joint angles are obtained by encoders and the sampling period of the control loop is 1 ms.

In order to validate the proposed grasping controller, a simple PD controller was used for the first joints of the fingers ($k_P = 0.9, k_D = 0.008$) keeping these joints stationary during the planar grasping experiments as validated by the acquired results.

Two types of objects were used in the experiments: a cube and a sphere, both of which were made of styrene foam. Their parameters are given in Table V. Moreover, in all cases, $k_{v_i} = 0.008$ for $i = 1, 2$ and $f_d = 1$.

Table IV. Motor and encoder specifications.

Maximum speed (rpm)	9550
Maximum torque (Nm)	257
Gear ratio	5.4 : 1
Resolution ($^{\circ}$)	0.0167

Table V. Parameters of the grasped objects.

Cube	
Mass (kg)	0.0021
Side length (m)	0.048
Sphere	
Mass (kg)	0.00019
Radius (m)	0.33

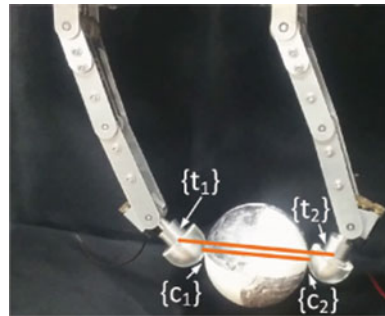


Fig. 21. Fingertip and interaction lines at equilibrium.

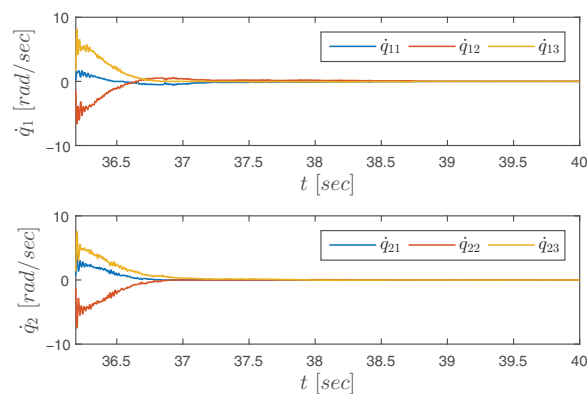


Fig. 22. Joint angular velocities of the prototype robotic hand.

As was previously shown in the theoretical analysis, the desired finger relative orientation parameter γ_s roughly defines the final relative orientation of the fingers which also depends on the geometry of the object and the deformation of the fingertips (27). Figures 19 and 20 show photographs of the initial and the equilibrium position achieved as well as the fingers' relative orientation response for the cube and the sphere and for all considered values of γ_s ($\gamma_s = 0^{\circ}$, $\gamma_s = 45^{\circ}$, $\gamma_s = 90^{\circ}$). It is clear that the desired relative finger orientation is roughly achieved. The small error in the relative orientation response in the cube case may be attributed to the tangential deformation of the fingertips

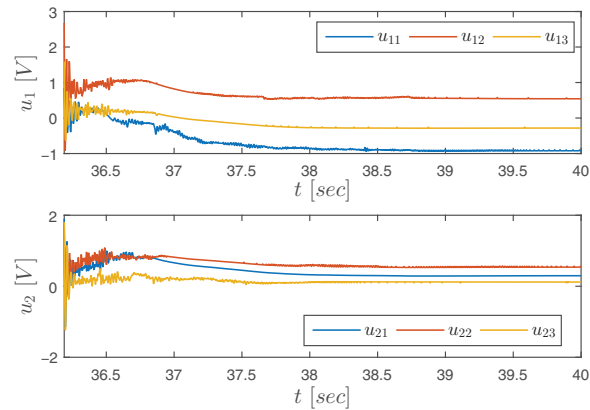


Fig. 23. Control input.

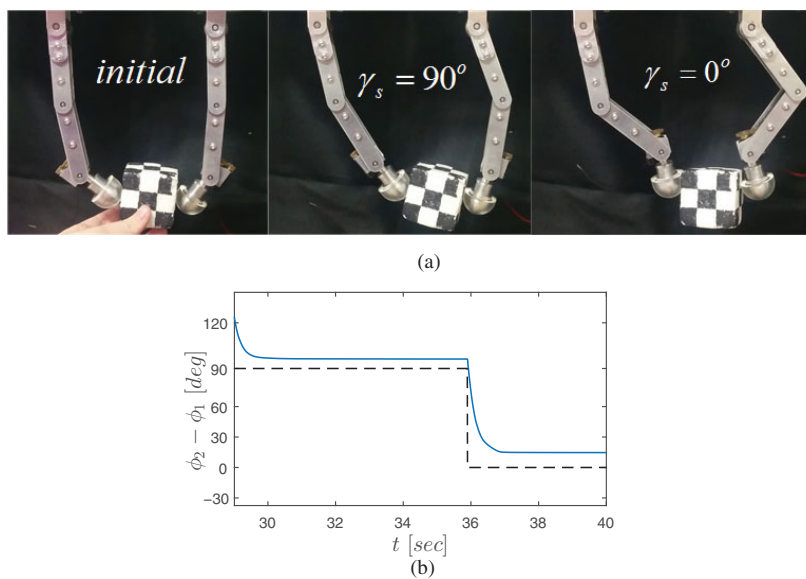


Fig. 24. Stable grasping of a cube transitioning from $\gamma_s = 90^\circ$ to $\gamma_s = 0^\circ$ (the dashed line corresponds to γ_s and the solid line to the relative finger orientation $\phi_2 - \phi_1$). (a) Finger relative orientation transition. (b) Relative finger orientation.

and the object weight, both of which are not taken into account in the theoretical equilibrium manifold without however compromising the stability of the system.

Figure 21 shows indicatively the equilibrium position of the system for the sphere with desired finger relative orientation $\gamma_s = 90^\circ$. It is clear that the fingertip line is parallel to the interaction line confirming the theoretical analysis. Moreover, the angular velocities of the fingers' joints converge to zero in all cases which shows that the object is stably grasped (Fig. 22) and the control input voltage stays well below the limit of 10 V (Fig. 23).

Finally, we demonstrate the experimental results of the transfer between one finger relative orientation to another with the use of the γ_s control parameter. Figures 24 and 25 show the transition of the system from the initial non-stable position to two successive desired relative fingertip orientations. Two different transitions are shown for the two objects, the transition of a cube from $\gamma_s = 90^\circ$ to $\gamma_s = 0^\circ$ (Fig. 24) and the transition of a sphere from $\gamma_s = 45^\circ$ to $\gamma_s = 90^\circ$ (Fig. 25). It is clear from the response of the relative finger orientation and the joint angular velocities, which converge to zero after the transition (Fig. 26), that the object remains stably grasped while achieving the desired finger shaping.

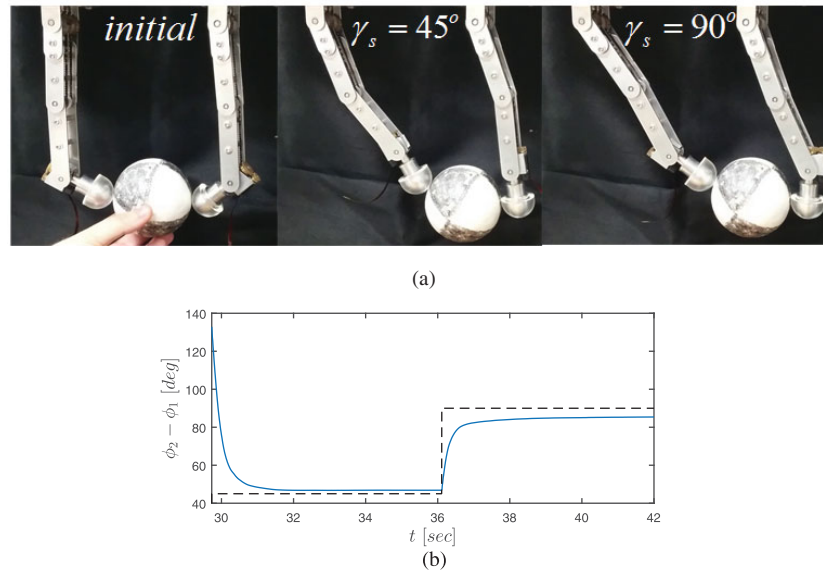


Fig. 25. Stable grasping of a sphere transitioning from $\gamma_s = 45^\circ$ to $\gamma_s = 90^\circ$ (the dashed line corresponds to γ_s and the solid line to the relative finger orientation $\phi_2 - \phi_1$). (a) Finger relative orientation transition. (b) Relative finger orientation.

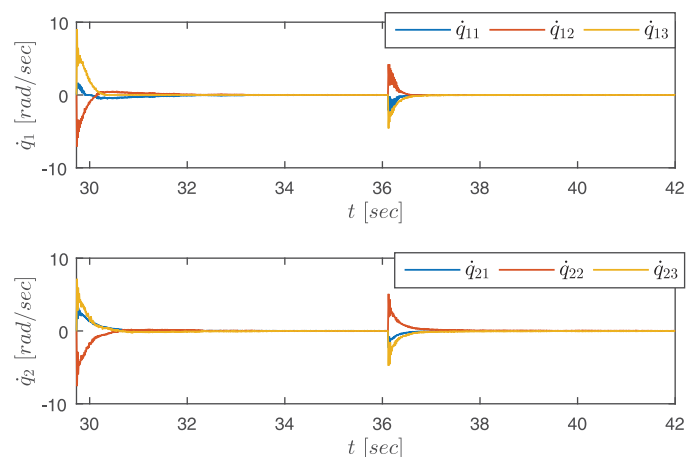


Fig. 26. Joint angular velocities with finger relative orientation transition.

8. Conclusions

In this paper, a grasping controller for an arbitrary-shaped object is proposed for two robotic fingers with soft tips. The controller does not require contact sensing while it adjusts the desired relative finger orientation allowing the shaping of the finger-object cluster for subsequent tasks or for increasing the grasping force manipulability. Grasp stability is theoretically justified and the equilibrium manifold is derived. The controller is validated via both simulations and experiments for objects with various shapes.

Acknowledgments

This research is co-financed by the EU-ESF and Greek national funds through the Operational Program "Education and Lifelong Learning" of the National Strategic Reference Framework (NSRF)-Research Funding Program ARISTEIA I.

Supplementary materials

For supplementary material for this article, please visit <https://doi.org/10.1017/S0263574717000303>.

References

1. M. T. Mason and J. K. Salisbury, *Robot Hands and the Mechanics of Manipulation* (MIT Press, Cambridge, MA, 1985).
2. H. Kawasaki, T. Komatsu and K. Uchiyama, "Dexterous anthropomorphic robot hand with distributed tactile sensor: Gifu hand II," *IEEE/ASME Trans. Mechatronics* **7**(3), 296–303 (2002).
3. K. Hoshino and I. Kawabuchi, "Pinching at fingertips for humanoid robot hand," *J. Robot. Mechatronics* **17**(6), 655–663 (2005).
4. H. Liu, K. Wu, P. Meusel, N. Seitz, G. Hirzinger, M. Jin, Y. Liu, S. Fan, T. Lan and Z. Chen, "Multisensory Five-Finger Dexterous Hand: The DLR/HIT Hand II," *IEEE/RSJ International Conference on Intelligent Robots and Systems* (Nice, France, Sep. 2008) pp. 3692–3697.
5. SHADOW, "Shadow dexterous hand," built by the Shadow Robot Company based in London, UK. <http://www.shadowrobot.com/products/dexterous-hand/>
6. M. Zribi, J. Chen and M. Mahmoud, "Coordination and control of multi-fingered robot hands with rolling and sliding contacts," *J. Intell. Robot. Syst.* **24**(2), 125–149 (1999).
7. S. Arimoto, *Control Theory of Multi-fingered Hands: A Modelling and Analytical-mechanics Approach for Dexterity and Intelligence* (Springer-Verlag, London Limited, London, 2008).
8. A. Bicchi, "Hands for dexterous manipulation and robust grasping: A difficult road toward simplicity," *IEEE Trans. Robot. Autom.* **16**(6), 652–662 (2000).
9. T. Wimbock, C. Ott, A. Abu-Schaffer and G. Hirzinger, "Comparison of object-level grasp controllers for dynamic dexterous manipulation," *Int. J. Robot. Res.* **31**(1), 3–23 (2011).
10. J. Bohg, A. Morales, T. Asfour and D. Kragic, "Data-driven grasp Synthesis—a survey," *IEEE Trans. Robot.* **30**(2), 289–309 (2013).
11. S. Farshchi, "Let's Bring Rosie Home: 5 Challenges We Need to Solve for Home Robots," In: *IEEE Spectrum's Automaton* (E. Guizzo, ed.) (2016). <http://spectrum.ieee.org/automaton/robotics/home-robots/lets-bring-rosie-home-5-challenges-we-need-to-solve-for-home-robots>
12. R. Murray and S. Sastry, *A Mathematical Introduction to Robotic Manipulation* (CRC Press INC, Boca Raton, Florida, USA, 1994).
13. A. Bicchi and V. Kumar, "Robotic Grasping and Contact: A Review," *IEEE International Conference on Robotics and Automation* (San Francisco, CA, USA, 2000) pp. 348–353.
14. D. Prattichizzo and J. C. Trinkle, "Grasping," In: *Springer Handbook of Robotics* (Prof. B. Siciliano and Prof. O. Khatib eds.) (Springer, Berlin, Heidelberg, 2008) pp. 671–700.
15. D. Prattichizzo, M. Malvezzi, M. Gabiccini and A. Bicchi, "On the manipulability ellipsoids of underactuated robotic hands with compliance," In: *Robot. Auton. Syst.* (Prof. B. Siciliano and Prof. O. Khatib, eds.) **60**(3), 337–346 (2012).
16. M. A. Roa and R. Suarez, "Computation of independent contact regions for grasping 3-D objects," *IEEE Trans. Robot.* **25**(4), 839–850 (2009).
17. R. Krug, D. Dimitrov, K. Charusta and B. Iliev, "On the Efficient Computation of Independent Contact Regions for Force Closure Grasps," *IEEE/RSJ International Conference on Intelligent Robots and Systems* (Taipei, Taiwan, Oct. 2010) pp. 586–591.
18. C. Rosales, R. Suarez, M. Gabiccini and A. Bicchi, "On the Synthesis of Feasible and Prehensile Robotic Grasps," *Proceedings of the 2012 IEEE International Conference on Robotics and Automation* (Saint Paul, MN, USA, May 2012) pp. 550–556.
19. A. Rodriguez, M. T. Mason and S. Ferry, "From Caging to Grasping," In: *Robotics: Science and Systems Conference (RSS)* (Los Angeles, Pittsburgh, PA, USA, 2011) pp. 1–8.
20. J. Seo, S. Kim and V. Kumar, "Planar, Bimanual, Whole-Arm Grasping," *IEEE International Conference on Robotics and Automation* (Saint Paul, MN, USA, May 2012) pp. 3271–3277.
21. L. Zhang and J. C. Trinkle, "The Application of Particle Filtering to Grasping Acquisition with Visual Occlusion and Tactile Sensing," *IEEE International Conference on Robotics and Automation* (Saint Paul, MN, USA, May 2012) pp. 3805–3812.
22. A. T. Miller and P. K. Allen, "GraspIt!" *IEEE Robot. Autom. Mag.* **11**(4), 110–122 (2004).
23. A. T. Miller, S. Knoop, H. I. Christensen and P. K. Allen, "Automatic Grasp Planning using Shape Primitives," *IEEE International Conference on Robotics and Automation* (Taipei, Taiwan, Sep. 2003) pp. 1824–1829.
24. R. Pelossof, A. Miller, P. Allen and T. Jebara, "An SVM Learning Approach to Robotic Grasping," *IEEE International Conference on Robotics and Automation* (New Orleans, LA, USA, Apr. 2004) pp. 3512–3518.
25. C. Goldfeder, P. K. Allen, C. Lackner and R. Pelossof, "Grasp Planning Via Decomposition Trees," *IEEE International Conference on Robotics and Automation* (Rome, Italy, Apr. 2007) pp. 4679–4684.
26. C. Borst, M. Fischer and G. Hirzinger, "Grasping the Dice by Dicing the Grasp," *IEEE/RSJ International Conference on Intelligent Robots and Systems* (Las Vegas, NV, USA, Oct. 2003) pp. 3692–3697.
27. M. T. Ciocarlie and P. K. Allen, "Hand posture subspaces for dexterous robotic grasping," *Int. J. Robot. Res.* **28**(7), 851–867 (2009).
28. R. Balasubramanian, L. Xu, P. D. Brook, J. R. Smith and Y. Matsuoka, "Physical human interactive guidance: Identifying grasping principles from human-planned grasps," *IEEE Trans. Robot.* **28**(4), 899–910 (2012).
29. J. Weisz and P. K. Allen, "Pose Error Robust Grasping from Contact Wrench Space Metrics," *IEEE International Conference on Robotics and Automation* (Saint Paul, MN, USA, May 2012) pp. 557–562.

30. D. Kappler, J. Bohg and S. Schaal, "Leveraging Big Data for Grasp Planning," *Proceedings of the IEEE International Conference on Robotics and Automation (ICRA)*, IEEE (Seattle, WA, USA, May 2015) pp. 4304–4311.
31. E. Johns, S. Leutenegger and A. J. Davison, "Deep Learning a Grasp Function for Grasping Under Gripper Pose Uncertainty," *Proceedings of the IEEE/RSJ International Conference on Intelligent Robots and Systems (IROS)*, IEEE, Daejeon, South Korea (Oct. 2016) pp. 4461–4468.
32. S. Arimoto, P. T. A. Nguyen, H.-Y. Han and Z. Doulgeri, "Dynamics and control of a set of dual fingers with soft tips," *Robotica* **18**(1), 71–80 (2000).
33. Z. Doulgeri, J. Fasoulas and S. Arimoto, "Feedback control for object manipulation by a pair of soft tip fingers," *Robotica* **20**(1), 1–11 (2002).
34. S. K. Song, J. B. Park and Y. H. Choi, "Dual-fingered stable grasping control for an optimal force angle," *IEEE Trans. Robot.* **28**(1), 256–262 (2012).
35. R. Ozawa, S. Arimoto and S. Nakamura, "Control of an object with parallel surfaces by a pair of finger robots without object sensing," *IEEE Trans. Robot.* **21**(5), 965–976 (2005).
36. S. Arimoto, "A differential-geometric approach for 2D and 3D object grasping and manipulation," *Annu. Rev. Control* **31**(2), 189–209 (2007).
37. S. Arimoto, K. Tahara, M. Yamaguchi, P. Nguyen and M.-Y. Han, "Principles of superposition for controlling pinch motions by means of robot fingers with soft tips," *Robotica* **19**(01), 21–28 (2001).
38. S. Arimoto, K. Tahara, J.-H. Bae and M. Yoshida, "A stability theory of a manifold: Concurrent realization of grasp and orientation control of an object by a pair of robot fingers," *Robotica* **21**(02), 163–178 (2003).
39. M. Yoshida, S. Arimoto and K. Tahara, "Pinching 2D Object with Arbitrary Shape by Two Robot Fingers Under Rolling Constraints," *IEEE/RSJ International Conference on Intelligent Robots and Systems* (St Louis, MO, USA, 2009) pp. 1805–1810.
40. A. Kawamura, K. Tahara, R. Kurazume and T. Hasegawa, "Dynamic grasping of an arbitrary polyhedral object," *Robotica* **31**(04), 511–523 (2013).
41. M. Grammatikopoulou, E. Psomopoulou, L. Droukas and Z. Doulgeri, "A Controller for Stable Grasping and Desired Finger Shaping without Contact Sensing," *IEEE International Conference on Robotics and Automation* (Hong Kong, China, May 2014) pp. 3662–3668.
42. K. Shimoga and A. Goldenberg, "Soft robotic fingertips part II: Modeling and impedance regulation," *Int. J. Robot. Res.* **15**(4), 335–350 (1996).
43. P. Chiacchio, S. Chiaverini, L. Sciavicco and B. Siciliano, "Global task space manipulability ellipsoids for multiple-arm systems," *IEEE Trans. Robot. Autom.* **7**(5), 678–685 (1991).
44. F. Caccavale and M. Uchiyama, "Cooperative Manipulators," **In: Springer Handbook of Robotics** (Prof. B. Siciliano and Prof. O. Khatib, eds.) (Springer, Berlin, Heidelberg, 2008) pp. 701–718.
45. T. Yoshikawa, *Foundations of Robotics* (MIT Press, Cambridge, MA, USA, 1990).
46. K. Tahara, K. Maruta, A. Kawamura and M. Yamamoto, "Externally Sensorless Dynamic Regrasping and Manipulation by a Triple-Fingered Robotic Hand with Torsional Fingertip Joints," *IEEE International Conference on Robotics and Automation* (Saint Paul, MN, USA, 2012) pp. 3252–3257.